JACS
JOURNAL OF THE AMERICAN CHEMICAL SOCIETY
Cite This: J. Am. Chem. Soc. 2019, 141, 7721−7725
Communication
pubs.acs.org/JACS

Using Redox-Active π Bridging Ligand as a Control Switch of Intramolecular Magnetic Interactions

Xiaozhou Ma,[†,‡] Elizaveta A. Suturina,[§] Mathieu Rouzières,[†,‡] Mikhail Platunov,[∥] Fabrice Wilhelm,[∥] Andrei Rogalev,[∥] Rodolphe Clérac,*[,†,‡] and Pierre Dechambenoit*[,†,‡]

[†]CNRS, CRPP, UMR 5031, Pessac F-33600, France
[‡]Univ. Bordeaux, CRPP, UMR 5031, Pessac F-33600, France
[§]Centre for Sustainable Chemical Technologies (CSCT), University of Bath, Claverton Down, Bath BA2 7AY, United Kingdom
[∥]ESRF-The European Synchrotron, CS 40220, 38043 Grenoble Cedex 9, France

Supporting Information

ABSTRACT: Intramolecular magnetic interactions in the dinuclear complexes $[(tpy)Ni(tphz)Ni(tpy)]^{n+}$ (n = 4, 3, and 2; tpy, terpyridine; tphz, tetrapyridophenazine) were tailored by changing the oxidation state of the pyrazine-based bridging ligand. While its neutral form mediates a weak antiferromagnetic (AF) coupling between the two S = 1 Ni(II), its reduced form, $tphz^{\bullet-}$, promotes a remarkably large ferromagnetic exchange of +214(5) K with Ni(II) spins. Reducing twice the bridging ligand affords weak Ni−Ni interactions, in marked contrast to the Co(II) analogue. Those experimental results, supported by a careful examination of the involved orbitals, provide a clear understanding of the factors which govern strength and sign of the magnetic exchange through an aromatic bridging ligand, a prerequisite for the rational design of strongly coupled molecular systems and high T_C molecule-based magnets.

Efficient control of the interactions between magnetic centers is a fascinating challenge, at the basis of any rational design of molecule-based magnets.[1] This fundamental problem is intrinsically linked to the question of the relative localization (or delocalization) of the unpaired electrons. Those are often located on d (or f) orbitals of metal ions, and they interact weakly by superexchange through diamagnetic bridging ligands or atoms. Nevertheless, alternative strategies have recently received an increasing interest to promote strong magnetic coupling: (i) the mixed-valence approach, for which an electron delocalization promotes double-exchange, which exceeds superexchange;[2] and (ii) the radical bridge approach using an organic radical ligand acting as a magnetic relay between paramagnetic metal centers.[3] For the latter, the organic bridge characteristics are crucial to optimize the strength of the magnetic interactions: it should be strongly coordinating for an efficient mixing of the involved metal/organic orbitals,[3d,4] and its unpaired electron as delocalized as possible between the paramagnetic metal ions.

Based on these prerequisites, our group reported recently[4] a prototype dinuclear complex based on Co(II) and the redox-active tphz bridging ligand.[5] In this system, the intramolecular magnetic interactions are controlled by successive reduction processes. While the neutral form of tphz mediates a weak AF exchange between *ls*-Co(II) (*ls*: low-spin), the once reduced radical form stabilizes very strong AF couplings between the S = 1/2 organic spin and the two *hs*-Co(II) (*hs*: high-spin). The resulting high-spin complex possesses a well isolated S_T = 5/2 ground state that is remarkably the only thermally populated state at ambient temperature. When further reducing this dinuclear complex, despite the formal diamagnetic state of the $tphz^{2-}$ ligand, a strong AF coupling between two *hs*-Co(II) is observed, leading to an overall nonmagnetic ground state. In this case, the strong magnetic interaction is induced by a large spin delocalization arising from an efficient orbital mixing of the $tphz^{2-}$ π system and one of the Co(II) singly occupied d orbitals. Therefore, in this type of radical/metal ion complexes, the nature and magnitude of the intramolecular coupling is indeed predictable based on both electronic configurations of metal ions and the bridging ligand.

To further experimentally investigate the role of the metal/organic orbital complementarity in the control of the magnetic interactions, a novel family of dinuclear Ni(II) complexes was synthesized with the redox-active tphz ligand. The reaction of $Ni(tpy)Cl_2$,[6] $TlPF_6$ and tphz in CH_3CN leads to a new dinuclear nickel complex that was isolated as orange needle-shaped crystals of $[Ni_2(tphz)(tpy)_2](PF_6)_4{\cdot}3CH_3CN$ (**1**) after slow diffusion of Et_2O vapors (Supporting Information, SI). The single crystal X-ray diffraction data at 120 K (Figure 1) reveal that **1** is isostructural to the Co(II) analogue,[5] possessing two equivalent $Ni^{II}(tpy)^{2+}$ fragments bridged by a neutral tphz ligand. The cyclic voltammetry of **1** in CH_3CN reveals four one-electron redox events at −0.40, −1.25, −1.66, and −1.82 V versus vs Fc^+/Fc (Figure 2)[7] with a rest potential at −0.15 V, indicating only reduction processes. By comparing with the reported Ru(II)[8] and Co(II)[4] analogues, the two processes at −0.40 and −1.25 V can be assigned to the reduction of the bridging ligand and the other two most cathodic ones to the tpy reduction. The large separation between the two first redox potentials evidence the high stability of the tphz radical in the complex, with a comproportionation constant of ca. 2.6×10^{14}. Based on these redox properties, **1** was chemically reduced with KC_8 to

Received: March 27, 2019
Published: April 26, 2019

Downloaded via STATE PUBLIC SCI TECHN LIB on May 29, 2020 at 12:37:39 (UTC).
See https://pubs.acs.org/sharingguidelines for options on how to legitimately share published articles.

ACS Publications © 2019 American Chemical Society

DOI: 10.1021/jacs.9b03044
J. Am. Chem. Soc. 2019, 141, 7721−7725

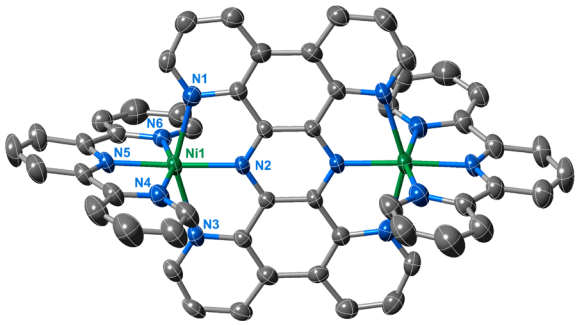

Figure 1. Crystal structure of $[Ni_2(tphz)(tpy)_2]^{4+}$ in **1** at 120 K (thermal ellipsoids: 50%). Hydrogen atoms, solvent molecules and anions are omitted for clarity.

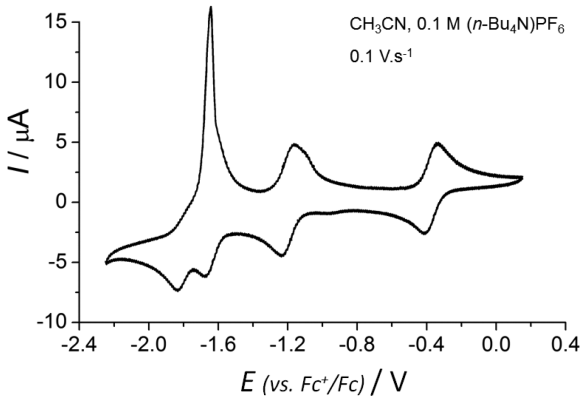

Figure 2. Cyclic voltammogram for a solution of **1**.

give once and twice-reduced systems as $[Ni_2(tphz)(tpy)_2](PF_6)_3{\cdot}2Et_2O$ (**2**) and $[Ni_2(tphz)(tpy)_2](PF_6)_2{\cdot}Et_2O$ (**3**) (SI) with similar coordination environments in the dinuclear cationic Ni(II) complexes (Figure S1 and Table S1). Nevertheless, significant differences are seen when comparing the bond distances within the bridging ligand (Tables 1 and S2) in agreement with two successive reductions as observed for the Co series.[4] In particular, C−N and N2···N2′ distances in the tphz pyrazine ring are significantly elongated, highlighting the successive reductions mainly centered on the bridging ligand. The Ni1−N2 distance decreases from 1.980(4) to 1.921(4) Å upon the two reductions as a result of the increasing electrostatic interactions between the cationic metal and the bridging ligand. Those bond distances are particularly short, but in perfect agreement with the reported cobalt series.[4] The average Ni−N bond distance involving terpyridine remains quasi-unchanged upon these two first reductions, indicating the tpy redox innocence and that the Ni ion preserved its spin state and charge in agreement with CASSCF calculations (Figure S4).[9]

Table 1. Selected Bond Distances (Å) in 1−3

	1	2	3
Ni−N1	2.268(5)	2.267(7)	2.305(4)
Ni−N2	1.980(4)	1.962(6)	1.921(4)
Ni−N3	2.336(5)	2.338(7)	2.326(4)
Ni−N4	2.089(5)	2.097(7)	2.100(4)
Ni−N5	1.975(4)	2.002(6)	1.997(3)
Ni−N6	2.078(5)	2.084(7)	2.114(4)
Ni−N(tpy)[a]	2.047(5)	2.061(7)	2.070(4)
C−C(pz)[a]	1.391(7)	1.384(10)	1.382(6)
C−N(pz)[ab]	1.331(7)	1.359(9)	1.375(6)

[a]pz: pyrazine part of tphz. [b]Average distance.

The local electronic and magnetic properties of the nickel metal ions were studied by X-ray absorption spectroscopy (XAS) and X-ray magnetic circular dichroism (XMCD). These techniques are particularly relevant for complexes with redox-active ligands, for which the oxidation state of the metal ion can be questioned.[10,11] The XAS spectrum at the Ni K-edge (Figure 3) is dominated by the $1s \rightarrow 4p$ transitions which show

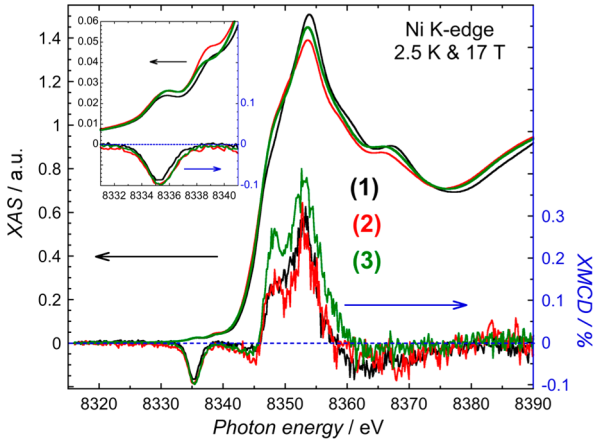

Figure 3. XAS and XMCD spectra. XAS spectra were normalized to zero before the edge and to unity far above the edge. XMCD spectra are given in XAS spectra %. Inset: magnification of the pre-edge region.

similar maxima for the three complexes between 8353.5 and 8353.8 eV. As expected for comparable coordination sphere of the probed atom, the first EXAFS (Extended X-ray Absorption Fine Structure) oscillations overlap remarkably well. The much weaker pre-edge, dipole-forbidden, $1s \rightarrow 3d$ transitions are detected at 8335.9 ± 0.2 and 8338.9 ± 0.3 eV for the three complexes in agreement with the expected and calculated Ni(II) ligand field splitting scheme (Figure S4).[11a] The XMCD experiments were also performed at the nickel K-edge to probe the Ni orbital magnetic moment (Figure 3). Considering that the spin−orbit interactions of the ligand atoms are negligibly small and thus cannot induce a significant orbital magnetic moment on the Ni centers, the observed XMCD signal at 8335.2 ± 0.1 eV is only due to the orbital polarization of the $4p$ and $3d$ states induced by the intra-atomic spin−orbit coupling of the Ni atoms. The Ni magnetic moment is thus directly proportional to the XMCD signals observed in the pre-edge and edge regions. Their quasi-identical intensities demonstrate the presence of the same magnetic moment and thus spin-state on the Ni metal ions in **1**−**3**. The similarity of the XAS and XMCD spectra establishes unambiguously the identical electronic and magnetic characteristics of the Ni site in these complexes.

To quantify the strength of the intramolecular magnetic coupling, dc magnetic measurements were performed at 0.1 T (Figure 4). The χT product of **1** remains constant between 300 and 80 K at 2.4 cm^3 K mol^{-1}, in good agreement with the presence of two $S = 1$ Ni(II) (C_{Ni} = 1.2 cm^3 K mol^{-1}; g_{Ni} = 2.19(5)). Below 80 K, the progressive decrease of χT, to a minimum value of 0.38 cm^3 K mol^{-1} at 1.85 K, is the result of the concerted effect of weak AF interactions between nickel

DOI: 10.1021/jacs.9b03044
J. Am. Chem. Soc. 2019, 141, 7721−7725

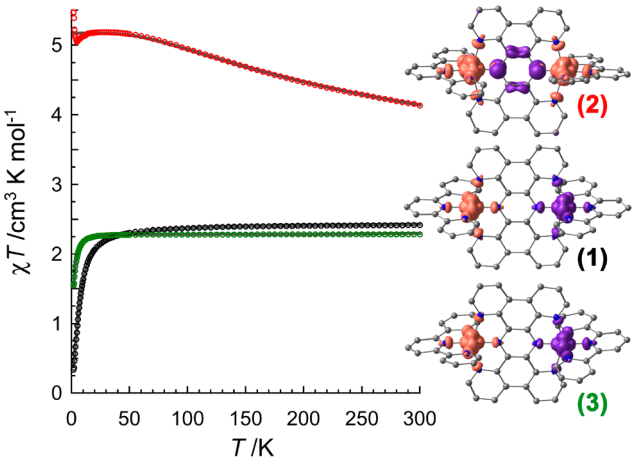

Figure 4. χT vs T plot at 0.1 T (gray lines: best fits; see text). Insets: View of the computed spin density.

spins and the Ni magnetic anisotropy. The fit of the experimental data with both contributions (solid lines, Figures 4 and S8)[12,13] gives g_{Ni} = 2.21(5), D_{Ni}/k_B = +13.6(3) K and J_{Ni-Ni}/k_B = −1.86(3) K comparable to −4.4 K obtained by broken-symmetry DFT (B3LYP/def2-TZVP) calculations (See SI for details).[9]

For the once-reduced analogue, **2**, the χT product at 300 K is 4.1 cm^3 K mol^{-1}, significantly higher than ca. 2.8 cm^3 K mol^{-1} expected for one S = 1/2 radical (g_{rad} = 2.0) and two Ni(II) (g_{Ni} = 2.2, S = 1 in agreement with XAS/XMCD). This result suggests a remarkably strong ferromagnetic exchange between the metal ion and the bridging radical tphz$^{\bullet-}$ spins that is confirmed by the χT increase between 300 and 40 K (Figures 4 and S9). Below 40 K, a χT plateau is reached with a maximum value of 5.2 cm^3 K mol^{-1}, which corresponds to an S_T = 5/2 ground state ($g_{S_T=5/2}$ = 2.18(5)). In this system, the ferromagnetic coupling is straightforward to rationalize considering the orthogonality of the Ni magnetic orbitals ($d_{x^2-y^2}$ and d_{z^2})[14] and the bridging ligand SOMO which is delocalized on the π system. Using an isotropic spin Heisenberg model,[15] its magnitude was estimated[13] to be $J_{Ni\text{-}rad}/k_B$ = +214(5) K (g = 2.17(5); Figure S9) leading to an energetically well isolated S_T = 5/2 ground state (the first S = 3/2 excited state lies at 214 K above). This large coupling is in good agreement with the calculated one (+249 K; DFT; SI),[9] and stronger than what was observed in other radical bridged Ni(II) complexes,[16] likely as a consequence of the strong metal−ligand coordination revealed by the short Ni−N2 bond.

For the twice-reduced compound **3**, the magnetic susceptibility data are similar to that for **1** with a constant χT product at ca. 2.3 cm^3 K mol^{-1} between 300 and 25 K (Figures 4 and S10), which is expected for a Curie behavior with two Ni(II) spins (g_{Ni} = 2.14(5)). As suggested by structural and spectroscopic measurements, the magnetic properties conclude unambiguously that the Ni oxidation and spin states do not change after successive reductions. Upon cooling below 25 K, the χT value decreases to 1.5 cm^3 K mol^{-1} at 1.85 K. Like in **1**, this low temperature behavior is probably the result of the combined contributions from the weak intramolecular AF interaction (−2.2 K from DFT)[9] and the Ni magnetic anisotropy. The χT vs T and M vs H fits[12,13] lead systematically to J_{Ni-Ni} values close to zero ($|J_{Ni-Ni}/k_B|$ < 0.1 K) with g_{Ni} = 2.14(5) and D_{Ni}/k_B = −10.4(3) K (solid lines in Figures 4 and S10). Despite the presence of a significant magnetic anisotropy, no out-of-phase ac signal was detected above 1.85 K and up to 10 kHz for these compounds.

This new series of complexes with different redox states offers the appealing opportunity for a direct comparison between Ni(II) and Co(II) analogues, for which only the metal electronic configuration differs. Indeed, the once- and twice-reduced forms of the Ni and Co complexes are quasi-isometric, providing a unique platform to directly probe the influence of the singly occupied atomic orbitals of the metal ion on the strength and sign of the magnetic coupling. According to the ab initio ligand field theory, the Ni(II) unpaired electrons are formally located on the $d_{x^2-y^2}$ and d_{z^2} orbitals (Figure S4),[14] which are only weakly interacting with tphz nitrogen σ-orbitals (Figures S5 and S7). In this situation, the spin density is, as expected, mostly located on the metal ions in **1** and **3** (Figure 4) and the magnetic interactions between the two Ni(II) spins are necessarily weak. Moreover, those metal ion singly occupied orbitals are orthogonal to the ligand π system. Therefore, as already mentioned, when the tphz$^{\bullet-}$ radical is stabilized in **2**, the unpaired electron is located on the ligand π orbital and a large ferromagnetic coupling is observed between metal and radical spins.

In *hs*-Co(II) analogues, in addition to the two unpaired electrons located on the $d_{x^2-y^2}$ and d_{z^2} orbitals, a third one is available on d_{xy}. This different configuration has a considerable impact on the magnetism,[4] as d_{xy} is the only orbital with an orientation that allows a significant overlap with the ligand π system. Hence, this efficient mixing of the d_{xy} and π orbitals induces an efficient spin density delocalization in the *hs*-Co(II) complexes. When twice-reduced, tphz^{2-} is formally diamagnetic, but the large spin delocalization promotes a strong AF coupling between the two Co(II) (−74 K), in striking contrast to **3**.[17] This comparative study demonstrates the key role of the d_{xy} orbital on the strength of the intramolecular magnetic exchange.

At least one order of magnitude is also gained on the magnetic interaction, when a single electron is located on the ligand π orbital. The metal ion and tphz$^{\bullet-}$ spins are strongly ferromagnetically coupled in the Ni(II) case with J/k_B = +214 K (vide supra), while a huge antiferromagnetic exchange is observed for the *hs*-Co(II) complex (at least −500 K). The $J(d_{xy}/\pi)$ coupling between the d_{xy} and π unpaired electrons is thus very large as it overcomes the ferromagnetic $J(d_{x^2-y^2}/\pi)$ and $J(d_{z^2}/\pi)$ contributions. Qualitatively, the $J(d_{xy}/\pi)$ interaction is thus larger than −700 K from the simple $J_{Co\text{-}rad}/k_B - J_{Ni\text{-}rad}/k_B$ relation.[18]

In conclusion, this work reports on a new series of dinuclear $[(tpy)Ni(tphz)Ni(tpy)]^{n+}$ complexes which provides, in comparison to the *hs*-Co(II) analogues, a complete set of experimental and theoretical results allowing a general understanding of the dominant factors governing the strength and nature of the magnetic coupling via an aromatic bridge. In particular, in addition to the obvious interest of using a radical bridging ligand, the careful selection of the metal ion based on its electronic configuration is the key step to promote the strongest possible coupling: this is happening when the unpaired electrons reside on the suitable t_{2g} orbitals, which overlap the best with the radical π system. This general

DOI: 10.1021/jacs.9b03044
J. Am. Chem. Soc. 2019, 141, 7721−7725

approach should be easily transposed to systems with higher nuclearities and dimensionalities, for which strong magnetic exchanges could be fully exploited to design high temperature molecule-based magnets.[10,19]

■ ASSOCIATED CONTENT

Supporting Information

The Supporting Information is available free of charge on the ACS Publications website at DOI: 10.1021/jacs.9b03044.

Experimental details about syntheses, structural, spectroscopic, magnetic characterizations and theoretical calculations (PDF)

X-ray crystallographic data for **1** (CIF)

X-ray crystallographic data for **2** (CIF)

X-ray crystallographic data for **3** (CIF)

■ AUTHOR INFORMATION

Corresponding Authors

*dechambenoit@crpp-bordeaux.cnrs.fr

*clerac@crpp-bordeaux.cnrs.fr

ORCID

Rodolphe Clérac: 0000-0001-5429-7418

Pierre Dechambenoit: 0000-0001-7850-2260

Notes

The authors declare no competing financial interest.

■ ACKNOWLEDGMENTS

This work was supported by the ANR (ANR-16-CE29-0001-01, Active-Magnet project), the University of Bordeaux, the Région Nouvelle Aquitaine, the CNRS, the MOLSPIN COST action CA15128 and the Chinese Scholarship Council (CSC) for the PhD funding of X.M.. E.A.S. thanks EPSRC for support (EP/N006895/1), the IRIDIS High Performance Computing Facility and associated services at the University of Southampton and RSC for travel grant. The authors thank also S. De, D. Woodruff, P. Perlepe, I. Oyarzabal, and S. Exiga for their assistance and fruitful discussions as well as the GdR MCM-2.

■ REFERENCES

(1) (a) Verdaguer, M.; Bleuzen, A.; Marvaud, V.; Vaissermann, J.; Seuleiman, M.; Desplanches, C.; Scuiller, A.; Train, C.; Garde, R.; Gelly, G.; Lomenech, C.; Rosenman, I.; Veillet, P.; Cartier, C.; Villain, F. Molecules to build solids: high T_C molecule-based magnets by design and recent revival of cyano complexes chemistry. *Coord. Chem. Rev.* **1999**, *190–192*, 1023–1047. (b) Weihe, H.; Güdel, H. U. Magnetic exchange across the cyanide bridge. *Comments Inorg. Chem.* **2000**, *22*, 75–103. (c) Ruiz, E.; Rodriguez-Fortea, A.; Alvarez, S.; Verdaguer, M. Is it possible to get high T_C magnets with Prussian blue analogues? A theoretical prospect. *Chem. - Eur. J.* **2005**, *11*, 2135–2144.

(2) (a) Bechlars, B.; D'Alessandro, D. M.; Jenkins, D. M.; Iavarone, A. T.; Glover, S. D.; Kubiak, C. P.; Long, J. R. High-spin ground states via electron delocalization in mixed-valence imidazolate-bridged divanadium complexes. *Nat. Chem.* **2010**, *2*, 362–368. (b) Gaudette, A. I.; Jeon, I.-R.; Anderson, J. S.; Grandjean, F.; Long, G. J.; Harris, T. D. Electron hopping through double-exchange coupling in a mixed-valence diiminobenzoquinone-Bridged Fe_2 Complex. *J. Am. Chem. Soc.* **2015**, *137*, 12617–12626.

(3) (a) Iwamura, H.; Inoue, K.; Hayamizu, T. High-spin polynitroxide radicals as versatile bridging ligands for transition metal complexes with high ferri/ferromagnetic T_C. *Pure Appl. Chem.* **1996**, *68*, 243–252. (b) Rinehart, J. D.; Fang, M.; Evans, W. J.; Long, J. R. A N_2^{3-} radical-bridged terbium complex exhibiting magnetic hysteresis at 14 K. *J. Am. Chem. Soc.* **2011**, *133*, 14236–14239. (c) Fortier, S.; Le Roy, J. J.; Chen, C.-H.; Vieru, V.; Murugesu, M.; Chibotaru, L. F.; Mindiola, D. J.; Caulton, K. G. A dinuclear cobalt complex featuring unprecedented anodic and cathodic redox switches for single-molecule magnet activity. *J. Am. Chem. Soc.* **2013**, *135*, 14670–14678. (d) Jeon, I.-R.; Park, J. G.; Xiao, D. J.; Harris, T. D. An azophenine radical-bridged Fe_2 single-molecule magnet with record magnetic exchange coupling. *J. Am. Chem. Soc.* **2013**, *135*, 16845–16848. (e) Demir, S.; Nippe, M.; Gonzalez, M. I.; Long, J. R. Exchange coupling and magnetic blocking in dilanthanide complexes bridged by the multi-electron redox-active ligand 2,3,5,6-tetra(2-pyridyl)pyrazine. *Chem. Sci.* **2014**, *5*, 4701–4711. (f) DeGayner, J. A.; Jeon, I.-R.; Harris, T. D. A series of tetraazalene radical-bridged M_2 ($M = Cr^{III}$, Mn^{II}, Fe^{II}, Co^{II}) complexes with strong magnetic exchange coupling. *Chem. Sci.* **2015**, *6*, 6639–6648. (g) Demir, S.; Jeon, I.-R.; Long, J. R.; Harris, T. D. Radical ligand-containing single-molecule magnets. *Coord. Chem. Rev.* **2015**, *289*, 149–176. (h) Moilanen, J. O.; Chilton, N. F.; Day, B. M.; Pugh, T.; Layfield, R. A. Strong exchange coupling in a trimetallic radical-bridged cobalt(II)-hexaazatrinaphthylene complex. *Angew. Chem., Int. Ed.* **2016**, *55*, 5521–5525. (i) Wang, J.; Li, J.-N.; Zhang, S.-L.; Zhao, X.-H.; Shao, D.; Wang, X.-Y. Syntheses and magnetic properties of a pyrimidyl-substituted nitronyl nitroxide radical and its cobalt(II) complexes. *Chem. Commun.* **2016**, *52*, 5033–5036. (j) Dolinar, B. S.; Gómez-Coca, S.; Alexandropoulos, D. I.; Dunbar, K. R. An air stable radical-bridged dysprosium single molecule magnet and its neutral counterpart: redox switching of magnetic relaxation dynamics. *Chem. Commun.* **2017**, *53*, 2283–2286. (k) Gould, C. A.; Darago, L. E.; Gonzalez, M. I.; Demir, S.; Long, J. R. A trinuclear radical-bridged lanthanide single-molecule magnet. *Angew. Chem., Int. Ed.* **2017**, *56*, 10103–10107. (l) Demir, S.; Gonzalez, M. I.; Darago, L. E.; Evans, W. J.; Long, J. R. Giant coercivity and high magnetic blocking temperatures for N_2^{3-} radical-bridged dilanthanide complexes upon ligand dissociation. *Nat. Commun.* **2017**, *8*, 2144. (m) Dolinar, B. S.; Alexandropoulos, D. I.; Vignesh, K. R.; James, T. A.; Dunbar, K. R. Lanthanide triangles supported by radical bridging ligands. *J. Am. Chem. Soc.* **2018**, *140*, 908–911. (n) Lemes, M. A.; Stein, H. N.; Gabidullin, B.; Robeyns, K.; Clérac, R.; Murugesu, M. Probing magnetic-exchange coupling in supramolecular squares based on reducible tetrazine-derived ligands. *Chem. - Eur. J.* **2018**, *24*, 4259–4253.

(4) Ma, X.; Suturina, E. A.; De, S.; Négrier, P.; Rouzières, M.; Clérac, R.; Dechambenoit, P. A redox-active bridging ligand to promote spin delocalization, high-spin complexes, and magnetic multi-switchability. *Angew. Chem., Int. Ed.* **2018**, *57*, 7841–7845.

(5) Iwamura, H.; Koga, N. Molecular approaches to photomagnetic materials. Metal-dependent regiospecificity in the exchange coupling of magnetic metal ions with free radical substituents on pyridine base ligands. *Pure Appl. Chem.* **1999**, *71* (2), 231–238.

(6) Lions, F.; Dance, I. G.; Lewis, J. Mono-chelate complexes of pyridine-2-aldehyde 2'-pyridylhydrazone. *J. Chem. Soc. A* **1967**, *0*, 565–572.

(7) The one electron process was confirmed by measuring the rest potential of solutions of **1** and **2**, −0.15 and −0.68 V respectively, prior recording their respective cyclic voltammograms, which were found to be identical.

(8) (a) Bonhôte, P.; Lecas, A.; Amouyal, E. Bi- and tri-nuclear ruthenium(II) complexes containing tetrapyridophenazine as a rigid bridging ligand. *Chem. Commun.* **1998**, *8*, 885–886. (b) Gourdon, A.; Launay, J.-P. Mononuclear and binuclear tetrapyrido[2,3-a:3',2'-c:2'',3''-h:3''',2'''-j]phenazine (tphz) ruthenium complexes. *Inorg. Chem.* **1998**, *37*, 5336–5341.

(9) Neese, F. The ORCA program system. *WIREs Comput. Mol. Sci.* **2012**, *2*, 73–78.

(10) Pedersen, K. S.; Perlepe, P.; Aubrey, M. L.; Woodruff, D. N.; Reyes-Lillo, S. E.; Reinholdt, A.; Voigt, L.; Li, Z.; Borup, K.; Rouzières, M.; Samohvalov, D.; Wilhelm, F.; Rogalev, A.; Neaton, J. B.; Long, J. R.; Clérac, R. Formation of the layered conductive magnet

DOI: 10.1021/jacs.9b03044
J. Am. Chem. Soc. 2019, 141, 7721–7725

$CrCl_2(pyrazine)_2$ through redox-active coordination chemistry. *Nat. Chem.* **2018**, *10*, 1056−1061.
(11) (a) Pickering, I. J.; George, G. N.; Lewandowski, J. T.; Jacobson, A. J. Nickel K-edge X-ray absorption fine structure of lithium nickel oxides. *J. Am. Chem. Soc.* **1993**, *115*, 4137−4144. (b) Szilagyi, R. K.; Lim, B. S.; Glaser, T.; Holm, R. H.; Hedman, B.; Hodgson, K. O.; Solomon, E. I. Description of the ground state wave functions of Ni dithiolenes using sulfur K-edge X-ray absorption spectroscopy. *J. Am. Chem. Soc.* **2003**, *125*, 9158−9169. (c) Perlepe, P.; Oyarzabal, I.; Pedersen, K. S.; Negrier, P.; Mondieig, D.; Rouzières, M.; Hillard, E. A.; Wilhelm, F.; Rogalev, A.; Suturina, E. A.; Mathonière, C.; Clérac, R. $Cr(pyrazine)_2(OSO_2CH_3)_2$: a two-dimensional coordination polymer with an antiferromagnetic ground state. *Polyhedron* **2018**, *153*, 248−253. (d) Liang, H. W.; Kroll, T.; Nordlund, D.; Weng, T.-C.; Sokaras, D.; Pierpont, C. G.; Gaffney, K. J. Charge and spin-state characterization of cobalt bis(o-dioxolene) valence tautomers using Co Kβ X-ray emission and L-Edge X-ray absorption spectroscopies. *Inorg. Chem.* **2017**, *56*, 737−747. (e) Koroidov, S.; Hong, K.; Kjaer, K. S.; Li, L.; Kunnus, K.; Reinhard, M.; Hartsock, R. W.; Amit, D.; Eisenberg, R.; Pemmaraju, C. D.; Gaffney, K.; Cordones, A. A. Probing the electron accepting orbitals of Ni-centered hydrogen evolution catalysts with noninnocent ligands by Ni L-edge and S K-edge X-ray absorption. *Inorg. Chem.* **2018**, *57*, 13167−13175. (f) Jafri, S. F.; Koumousi, E. S.; Arrio, M.-A.; Juhin, A.; Mitcov, D.; Rouzières, M.; Dechambenoit, P.; Li, D.; Otero, E.; Wilhelm, F.; Rogalev, A.; Joly, L.; Kappler, J.-P.; Moulin, C. C. D.; Mathonière, C.; Clérac, R.; Sainctavit, P. Atomic scale evidence of the switching mechanism in a photomagnetic CoFe dinuclear Prussian blue analogue. *J. Am. Chem. Soc.* **2019**, *141*, 3470−3479.
(12) The following Hamiltonian has been used to fit the magnetic data:

$$\hat{H} = -2J_{Ni-Ni}(\vec{S}_{Ni1}\cdot\vec{S}_{Ni2}) + 2D_{Ni}S_{Ni,z}{}^2 + 2g_{Ni}\mu_B\vec{S}_{Ni}\cdot\vec{H}$$

(13) Chilton, N. F.; Anderson, R. P.; Turner, L. D.; Soncini, A.; Murray, K. S. PHI: a powerful new program for the analysis of anisotropic monomeric and exchange-coupled polynuclear d- and f-block complexes. *J. Comput. Chem.* **2013**, *34*, 1164−1175.
(14) The average N1−Ni−N3 axis is taken as the z direction by convention (Figure 1).
(15) The following Hamiltonian has been used to fit the magnetic data:

$$\hat{H} = -2J_{Ni-rad}(\vec{S}_{Ni1} + \vec{S}_{Ni2})\cdot\vec{S}_{rad} + \mu_B(2g_{Ni}\vec{S}_{Ni} + g_{rad}\vec{S}_{rad})\cdot\vec{H}$$

(16) (a) Dei, A.; Gatteschi, D.; Pardi, L. Sextet ground state in a dinuclear nickel(II) complex containing a tetraoxolene radical as bridging ligand. *Inorg. Chim. Acta* **1991**, *189*, 125−128. (b) Woods, T. J.; Stout, H. D.; Dolinar, B. S.; Vignesh, K. R.; Ballesteros-Rivas, M. F.; Achim, C.; Dunbar, K. R. Strong ferromagnetic exchange coupling mediated by a bridging tetrazine radical in a dinuclear nickel complex. *Inorg. Chem.* **2017**, *56*, 12094−12097. (c) Lemes, M. A.; Brunet, G.; Pialat, A.; Ungur, L.; Korobkov, I.; Murugesu, M. Strong ferromagnetic exchange coupling in a $\{Ni^{II}_4\}$ cluster mediated through an air-stable tetrazine-based radical anion. *Chem. Commun.* **2017**, *53*, 8660−8663.
(17) This is further confirmed by UV−vis-NIR spectrometry which reveals the absence of an absorption band in the NIR region for **3** (Figure S3) in contrast to its Co analogue (ref 4).
(18) More accurately, this $J(d_{xy}/\pi)$ antiferromagnetic coupling is better described as being between the $d_{xy}(Co) + \pi(N_{tphz})$ orbital and the π system of the carbon atoms of the tphz pyrazine part (for symmetry reasons of the involved orbitals).
(19) (a) Manriquez, J. M.; Yee, G. T.; McLean, R. S.; Epstein, A. J.; Miller, J. S. A room-temperature molecular/organic-based magnet. *Science* **1991**, *252*, 1415−1417. (b) Miller, J. S. Magnetically ordered molecule-based materials. *Chem. Soc. Rev.* **2011**, *40*, 3266−3296. (c) Miller, J. S.; Ohkoshi, S.-i. In *High-T_C Ordered Molecular Magnets in Molecular Magnetic Materials: Concepts and Applications*; Sieklucka, B., Pinkowicz, D., Eds.; Wiley-VCH: Wienheim, 2017.

DOI: 10.1021/jacs.9b03044
J. Am. Chem. Soc. 2019, 141, 7721−7725